Received: 15 January 2019 | Revised: 5 May 2019 | Accepted: 6 May 2019
DOI: 10.1002/aoc.5013

FULL PAPER

WILEY Applied Organometallic Chemistry

Containing-PMBP N_2O_2-donors transition metal(II) complexes: Synthesis, crystal structure, Hirshfeld surface analyses and fluorescence properties

Quan-Peng Kang | Xiao-Yan Li | Lan Wang | Yang Zhang | Wen-Kui Dong

School of Chemical and Biological Engineering, Lanzhou Jiaotong University, Lanzhou 730070, China

Correspondence
Wen-Kui Dong, School of Chemical and Biological Engineering, Lanzhou Jiaotong University. Lanzhou 730070, China.
Email: dongwk@126.com

Funding information
Program for Excellent Team of Scientific Research in Lanzhou Jiaotong University, Grant/Award Number: 201706; National Natural Science Foundation of China, Grant/Award Number: 21761018

Three newly designed containing-PMBP N_2O_2-donors complexes, $[Co(L^1)(CH_3OH)_2]$ (**1**), $[\{Zn(L^2)(CH_3OH)(H_2O)\}_3]$ (**2**) and $[Cu_4(L^2)_4]\cdot 2CHCl_3$ (**3**), have been synthesized and structurally characterized using elemental analyses, infrared and UV–visible spectroscopies and single-crystal X-ray diffraction. X-ray crystal structure determinations revealed that **1** consists of one Co(II) atom, one completely deprotonated $(L^1)^{2-}$ unit and two coordinated methanol molecules. Complex **2** consists of three Zn(II) atoms, three completely deprotonated $(L^2)^{2-}$ units, three coordinated methanol molecules and three coordinated water molecules. However, **3** includes four Cu(II) atoms, four completely deprotonated $(L^2)^{2-}$ units and two crystallization chloroform molecules. The Co(II) and Zn(II) atoms in the structures of **1** and **2** adopt slightly distorted octahedral geometries. While, Cu(II) atoms in **3** can be best described as adopting slightly distorted square planar geometries. Complex **2** is a novel structure, and the ratio of H_2L^2 to Zn(II) atom is 3:3. In addition, two-, three- and three-dimensional supramolecular structures were constructed for **1**, **2** and **3**. Most importantly, Hirshfeld surface analysis of **1**, **2** and **3** was conducted and fluorescence properties were investigated.

KEYWORDS
complex, crystal structure, fluorescence property, N_2O_2 donor ligands, synthesis

1 | INTRODUCTION

A Salen-like compound is a multifunctional tetradentate N_2O_2 chelating ligand in modern coordination chemistry.[1–6] A great number of metal coordination compounds with Salen-like N_2O_2 ligands have been extensively studied for several decades, which have been variously investigated for potential applications in biological fields,[7–12] electrochemical conduction,[13–15] ion recognitions,[16–21] supramolecular architectures,[22–26] catalysts,[27–29] as well as magnetic[30–35] and luminescent[36–41] materials. More recently, Salamo-like N_2O_2 chelating ligands and their analogues have been explored using an *O*-alkyloxime ($-CH{=}N{-}O{-}(CH_2)_n{-}O{-}N{=}CH{-}$). When an *O*-alkyloxime unit substitutes an imine moiety, the larger electronegativity of the oxygen atoms will improve significantly the electronic behaviors of the N_2O_2 coordination sphere, which may lead to novel structures and better properties of metal complexes.[42,43] A study has shown that these are at least 10^4 times more stable than Salen-like complexes.[44] In the work reported herein, three new complexes, $[Co(L^1)(CH_3OH)_2]$ (**1**), $[\{Zn(L^2)(CH_3OH)(H_2O)\}_3]$ (**2**) and $[Cu_4(L^2)_4]\cdot 2CHCl_3$ (**3**), constructed from Salamo-like N_2O_2 donor ligands were prepared and characterized structurally.

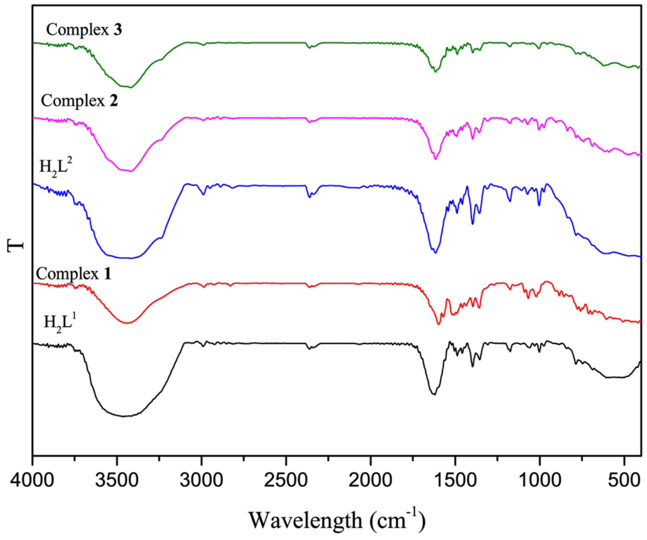

FIGURE 1 IR spectra of H_2L^1 and H_2L^2 and their complexes **1**, **2** and **3**

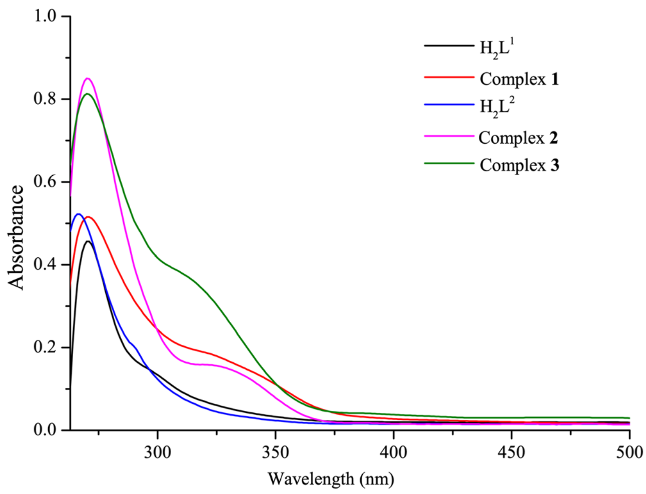

FIGURE 2 UV–visible spectra of H_2L^1 and H_2L^2 and their complexes **1**, **2** and **3**

2 | RESULTS AND DISCUSSION

2.1 | Infrared (IR) spectra analyses

The IR spectra of H_2L^1 and H_2L^2 and their complexes **1**, **2** and **3** show various absorption bands in the 4000–400 cm^{-1} region (Figure 1). It is obvious that typical broad ν(O—H) stretching bands were observed at 3454 and 3461 cm^{-1} in the spectra of H_2L^1 and H_2L^2, respectively. It is inferred that PMBP molecules in the ligands H_2L^1 and H_2L^2 exist in the enol form. The C=N stretching bands of ligands H_2L^1 and H_2L^2 appear at 1624 and 1619 cm^{-1}, and the spectra of complexes **1**, **2** and **3** show C=N stretching bands at 1605, 1608 and 1615 cm^{-1}, respectively.[45,46] The characteristic C=N stretching frequencies are shifted to lower values, indicating that the Co(II), Zn(II) and Cu(II) atoms are coordinated with the free ligands H_2L^1 and H_2L^2. The IR spectra of free ligands H_2L^1 and H_2L^2 show absorption bands at 1182 and 1179 cm^{-1}, assignable to Ar—O stretching. Compared with H_2L^1 and H_2L^2, the typical Ar—O stretching bands of complexes **1**, **2** and **3** occurred at 1175, 1175 and 1173 cm^{-1}, respectively. This phenomenon can be explained by the formation of M—O bonds (M = Co, Zn and Cu).[47] Meanwhile, the free ligand H_2L^1 exhibited typical aromatic C=C skeleton vibrations bands at 1505, 1487 and 1459 cm^{-1}, while for complex **1** these appeared at 1519, 1505 and 1489 cm^{-1}, respectively. The free ligand H_2L^2 also shows aromatic C=C skeleton vibration bands at 1521, 1486 and 1459 cm^{-1}, while those of complex **2** (or **3**) appear at 1519, 1492 and 1456 cm^{-1} (or 1507, 1487 and 1458 cm^{-1}), respectively.

2.2 | UV–visible absorption spectra

The UV–visible absorption spectra of H_2L^1 and H_2L^2 with those of their complexes **1**, **2** and **3** in dimethylformamide

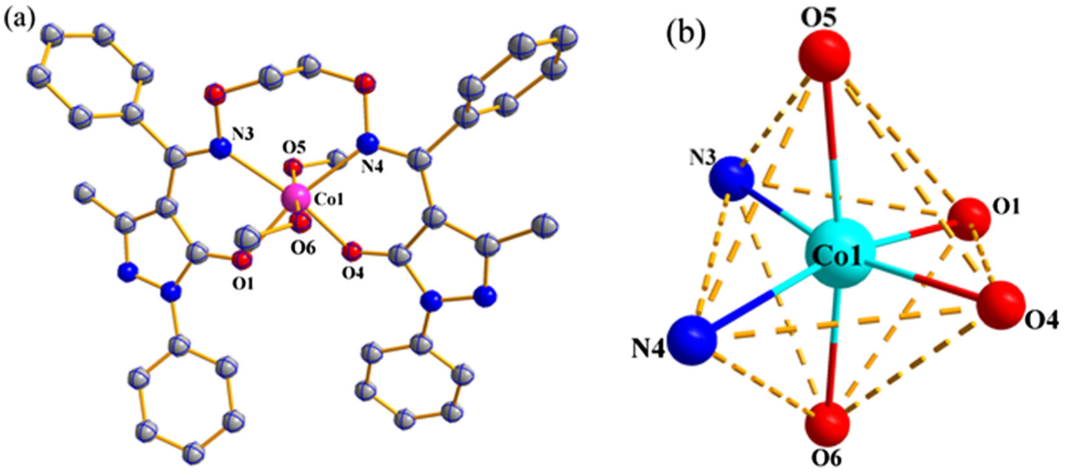
(a)
(b)

FIGURE 3 (a) View of the molecular structure of complex **1**. (b) Coordination polyhedron for the Co(II) atom of complex **1**

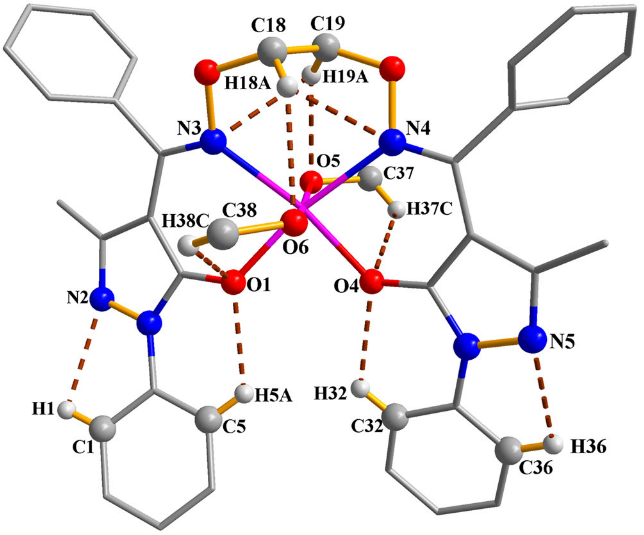

FIGURE 4 View of the intramolecular hydrogen bondings of complex **1**

(DMF) solution (1.0×10^{-5} M) at 298 K are shown in Figure 2. As the UV–visible absorption spectra of complexes **1**, **2** and **3** are similar, we obtain the same conclusion. The absorption spectra of the free ligands H_2L^1 and H_2L^2 exhibit relatively intense absorption peaks at *ca* 269 and 266 nm, respectively. These absorption peaks could be attributed to the π–π* type transitions of the benzene rings.[48] Compared to the absorption peaks of the free ligands H_2L^1 and H_2L^2, these absorption peaks of complexes **1**, **2** and **3** are bathochromically shifted to 270, 269 and 271 nm, respectively, indicating the coordination of Co(II), Zn(II) and Cu(II) atoms with the $(L^1)^{2-}$ or $(L^2)^{2-}$ units.[49,50] Meanwhile, new weak broad absorption peaks emerge at *ca* 314, 320 and 309 nm in the spectra of complexes **1**, **2** and **3**, respectively, which are attributed to the n–π* charge transfer transitions from the lone-pair electrons of the N atoms of C═N groups.[51]

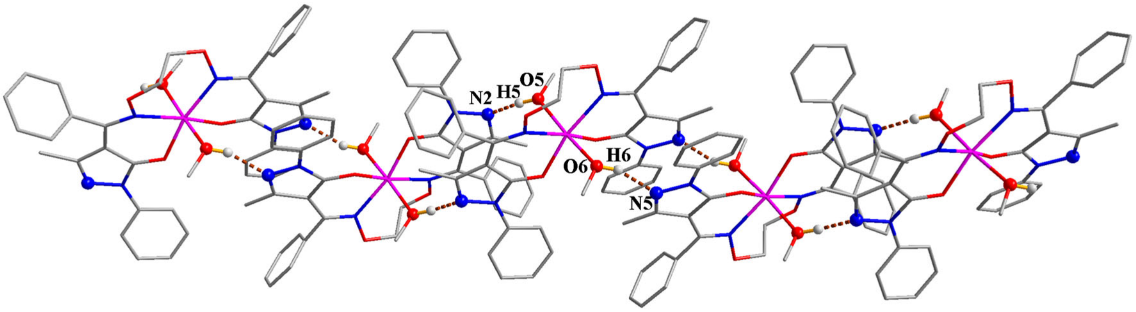

FIGURE 5 Part of the infinite one-dimensional supramolecular chain of complex **1**

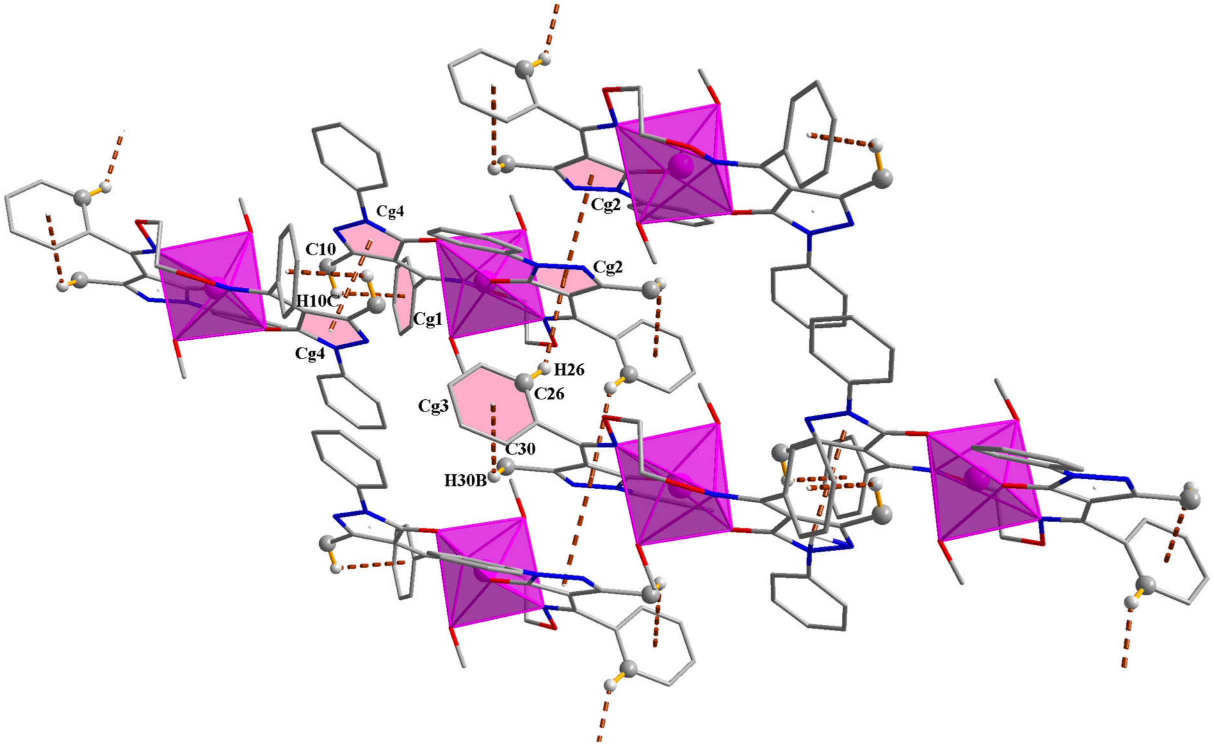

FIGURE 6 View of the two-dimensional supramolecular structure of complex **1** showing the C–H⋯π and π⋯π interactions

2.3 | Crystal structure of complex 1

The structure of complex **1** is shown in Figure 3. Selected bond lengths and angles are given in Table S1. The complex $[Co(L^1)(CH_3OH)_2]$ was isolated, and crystallizes in the triclinic system, space group *P*-1, with *Z* = 2. In the Co(II) complex, the molecule consists of one Co(II) atom, one completely deprotonated $(L^1)^{2-}$ unit and two coordinated methanol molecules at the two axial sites, resulting in a mononuclear Co(II) complex. The four atoms of the donor set (N3, N4, O1, O4) and Co1 essentially lie in a plane. The data for Co1–O1 (2.049(3) Å), Co1–O4 (2.051(3) Å), Co1–O5 (2.113(4) Å), Co1–O6 (2.116(4) Å), Co1–N3 (2.224(4) Å) and Co1–N4 (2.220(4) Å) revealed that the oxygen and nitrogen atoms take part in coordination with the Co(II) atom. The

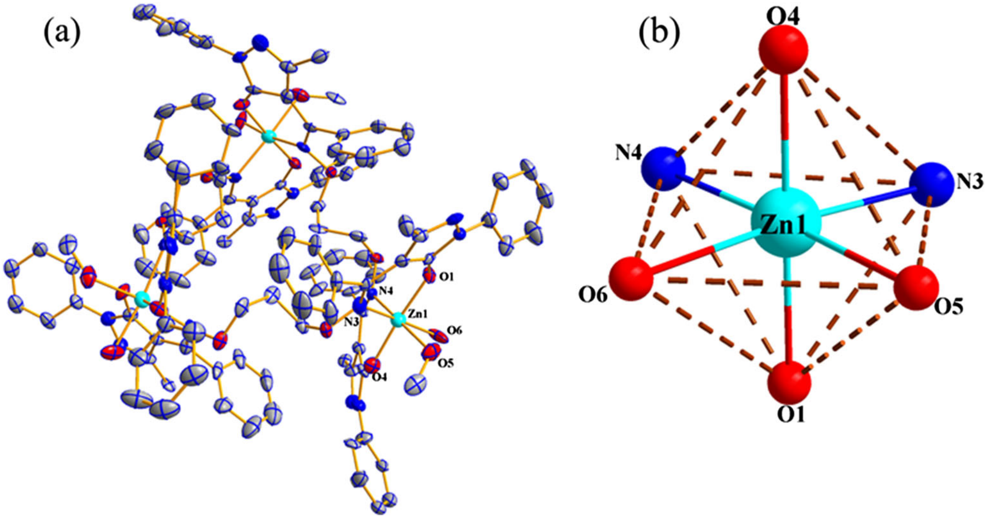

FIGURE 7 (a) Molecule structure of complex **2** (hydrogen atoms and solvent molecules are omitted for clarity). (b) Coordination polyhedron for Zn(II) atoms of complex **2**

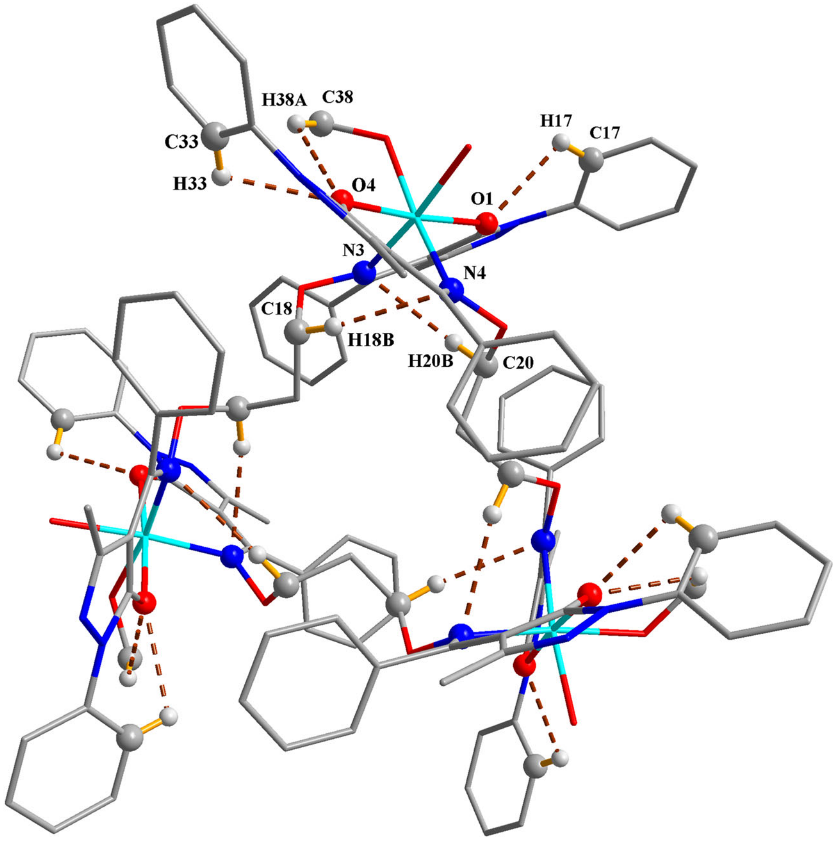

FIGURE 8 View of the intramolecular hydrogen bondings of complex **2**

dihedral angle between the two coordination planes, N3–Co1–O1 and N4–Co1–O4, is 10.62(9)°, indicating the coordination geometry around the central Co(II) atom is a slightly distorted octahedron.

In the crystal structure of complex **1**, there are ten significant intramolecular hydrogen bondings (C1–H1···N2, C5–H5A···O1, C18–H18A···O6, C18–H18A···N4, C19–H19A···O5, C19–H19A···N3, C32–H32···O4, C36–H36···N5, C37–H37C···O4 and C38–H38C···O1) and two intermolecular hydrogen bondings (O5–H5···N2 and O6–H6···N5), which perform a crucial role in constructing and stabilizing the supramolecular structure[52–54] (Figure 4). The units are interlinked by the intermolecular hydrogen bonding interactions into an infinite one-dimensional chain supramolecular structure (Figure 5). In addition, complex **1** molecules are interlinked effectively via three pairs of C–H···π (C10–H10C···Cg1, C26–H26···Cg2 and C30–H30B···Cg3) hydrogen bonding interactions and two pairs of π···π (Cg2···Cg2 and Cg4···Cg4) stacking interactions (Cg2 = N5–N6–C27–

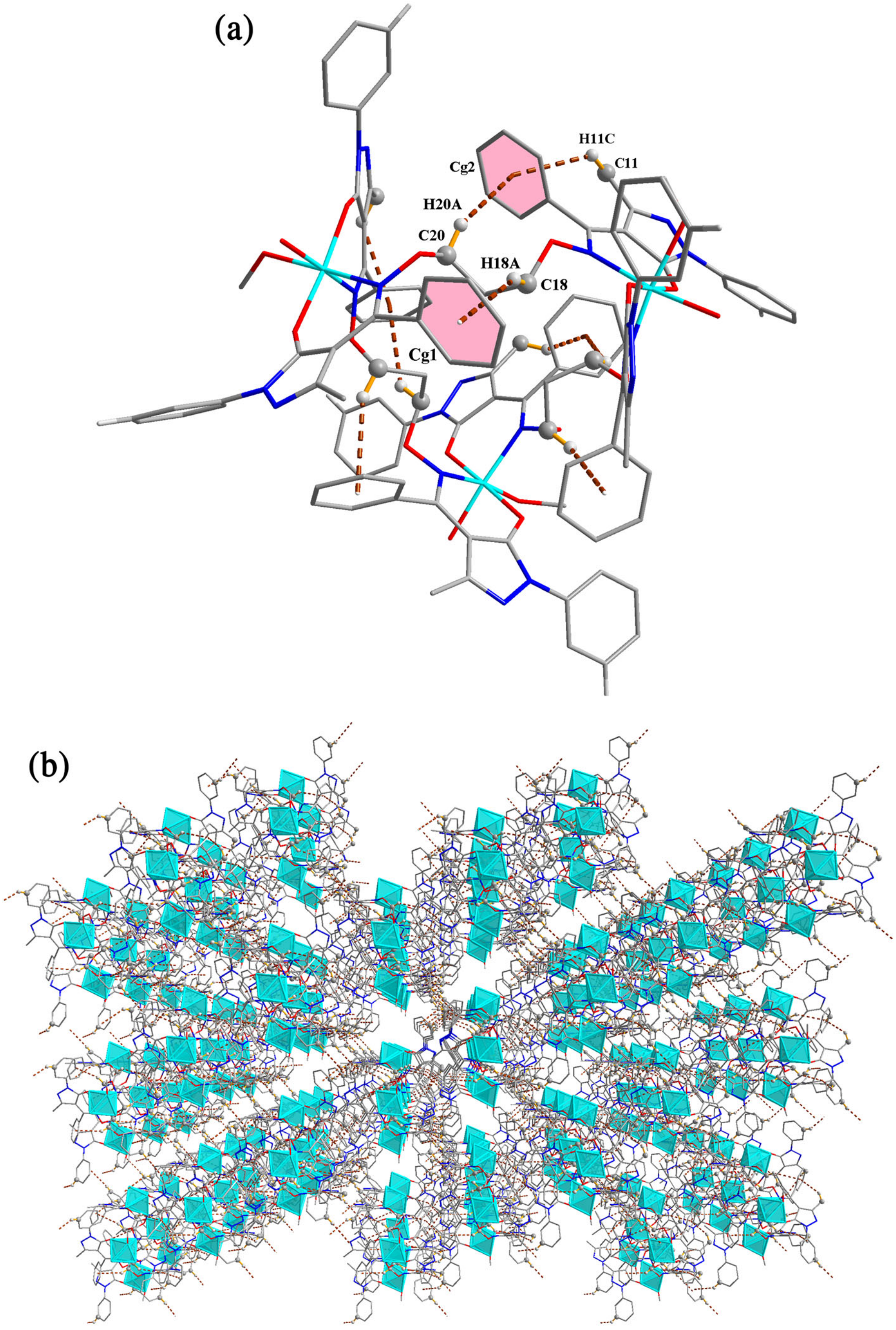

FIGURE 9 (a) View of the intramolecular hydrogen bondings and (b) three-dimensional supramolecular structure of complex **2** showing C–H···π hydrogen bonding interactions

C28–C29 and Cg4 = N1–N2–C7–C8–C9), which form an infinite two-dimensional layered supramolecular structure (Figure 6). The hydrogen bonding parameters are summarized in Table S2.

2.4 | Crystal structure of complex 2

The crystal structure of complex **2** is shown in Figure 7. Selected bond lengths and angles are given in Table S3. A colorless crystalline complex of rarely reported 3:3 complex $[\{Zn(L^2)(CH_3OH)(H_2O)\}_3]$ was isolated, and crystallizes in the trigonal system, space group $R3$, with $Z = 3$. The molecular structure of complex **2** consists of three Zn(II) atoms, three completely deprotonated $(L^2)^{2-}$ units, and three coordinated methanol and three coordinated water molecules. The three Zn(II) atoms are located in the N_2O_2 coordination spheres, and hexa-coordinated with donor N_2O_2 atoms and two other oxygen atoms (O5 and O6) come from the coordinated methanol and water molecules occupying the axial positions, respectively. The dihedral angle between coordination planes of N4–Zn1–O4 and N3–Ni1–O1 is 80.88(5)°, which indicates that the Zn(II) atoms form distorted octahedral geometries. The primary Zn–N and Zn–O distances are in the normal ranges (Zn1–O1 = 1.983(7), Zn1–O5 = 2.099(8), Zn1–O6 = 2.078(8), Zn1–O4$^{\#1}$ = 1.956(8), Zn1–N3 = 2.115(8) and Zn1–N4$^{\#1}$ = 2.111(8) Å) (Table S3). These data revealed that the oxygen and nitrogen atoms take part in coordination

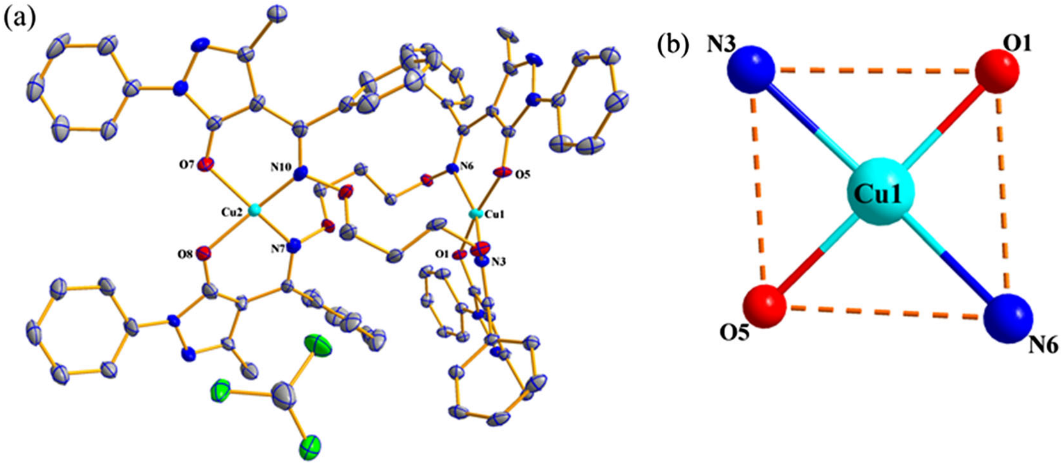

FIGURE 10 (a) Molecule structure of complex **3** (hydrogen atoms and solvent molecules are omitted for clarity). (b) Coordination polyhedron for Cu(II) atoms of complex **3**

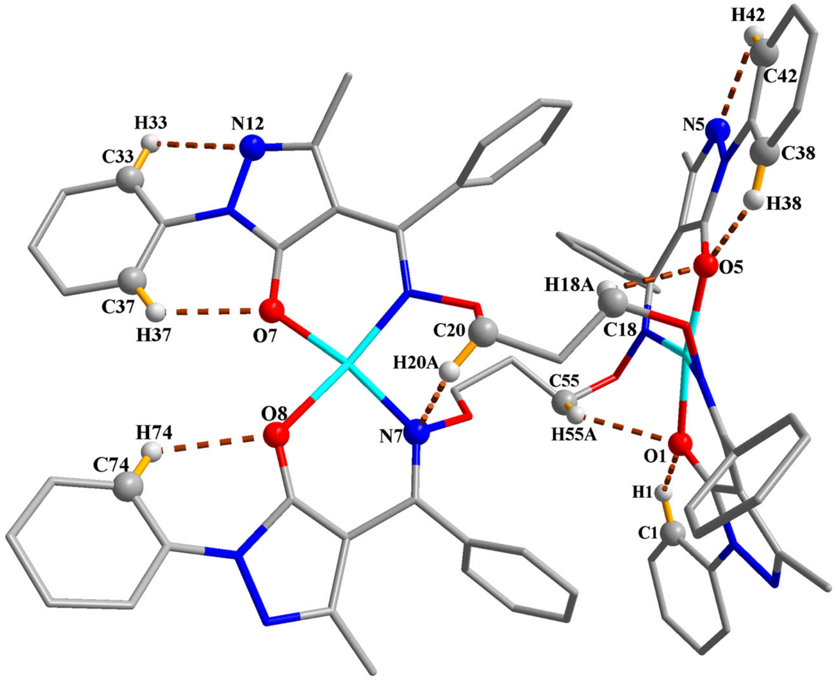

FIGURE 11 View of the intramolecular hydrogen bondings of complex **3**

with the Zn(II) atoms. The bond lengths between the Zn(II) atom and the apical oxygen atoms (O5 and O6) are 2.099(8) and 2.078(8) Å, which are obviously longer than the distances between the Zn(II) atom and the basal oxygen and nitrogen atoms. This significant elongation has been observed previously in Zn(II) complexes with Salamo-type ligands.

It is worth noting that the center of complex **2** has a similar cage-like geometry. The three Zn(II) atoms are connected through trialkylene chains, resulting in a 24-membered ring, which means that complex **2** has better stability.

As illustrated in Figure 8, in the crystal structure of complex **2**, the structure is connected by five pairs of intramolecular hydrogen bonding interactions (C17–H17···O1, C18–H18B···N4, C20–H20B···N3, C33–H33···O4 and C38–H38A···O4), which play a vital role in constructing and stabilizing complex **2**. In addition, there are three pairs of intramolecular C–H···π (C18–H18A···Cg1, C11–H11C···Cg2 and C20–H20A···Cg2) and

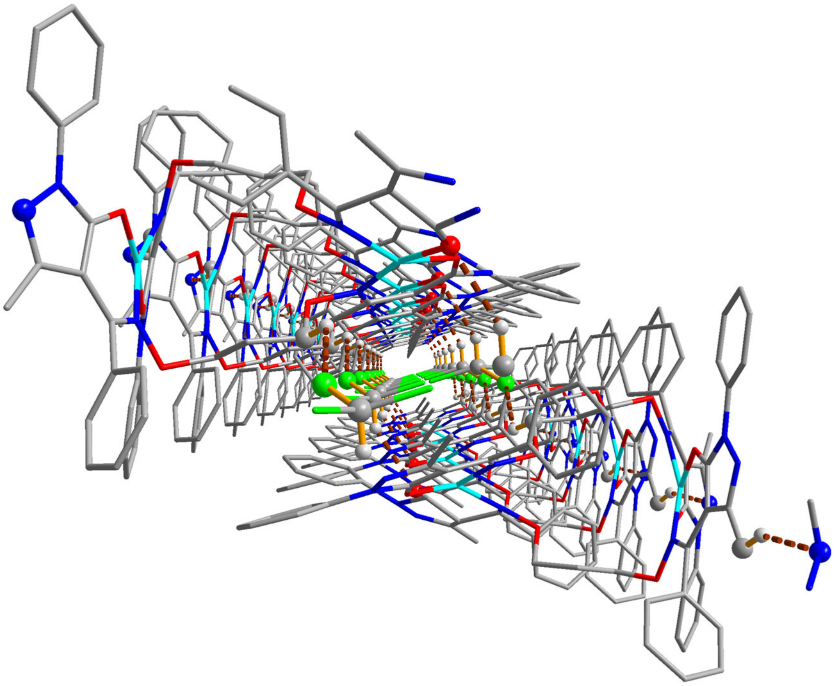

FIGURE 12 View of the three-dimensional supramolecular structure of complex **3** exhibiting intermolecular hydrogen bonding interactions

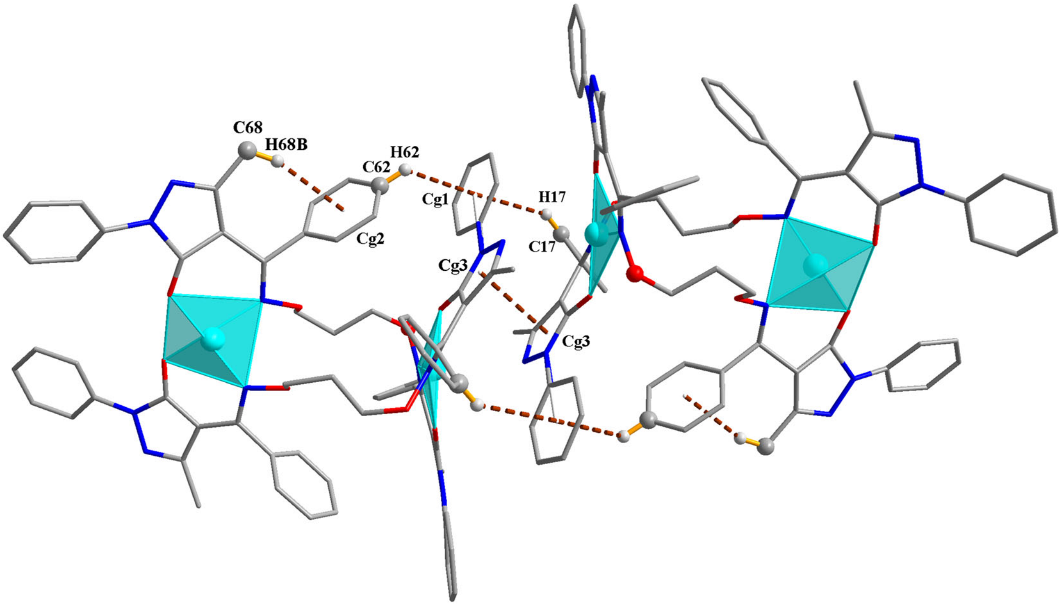

FIGURE 13 View of the one-dimensional structure of complex **3** exhibiting C–H···π hydrogen bonding and π···π stacking interactions

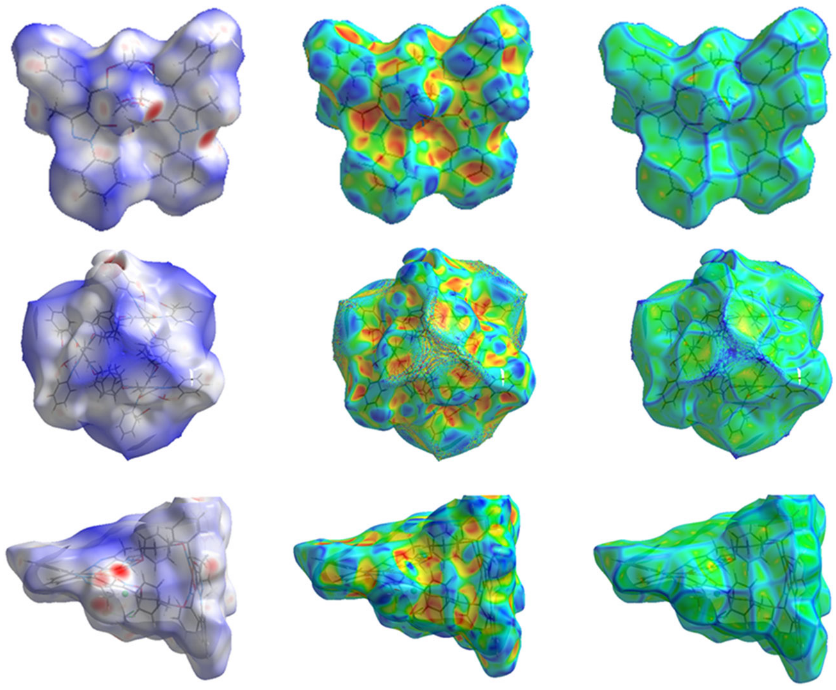

FIGURE 14 Hirshfeld surfaces mapped with d_{norm} (left), shape_index (middle) and curvedness (right)

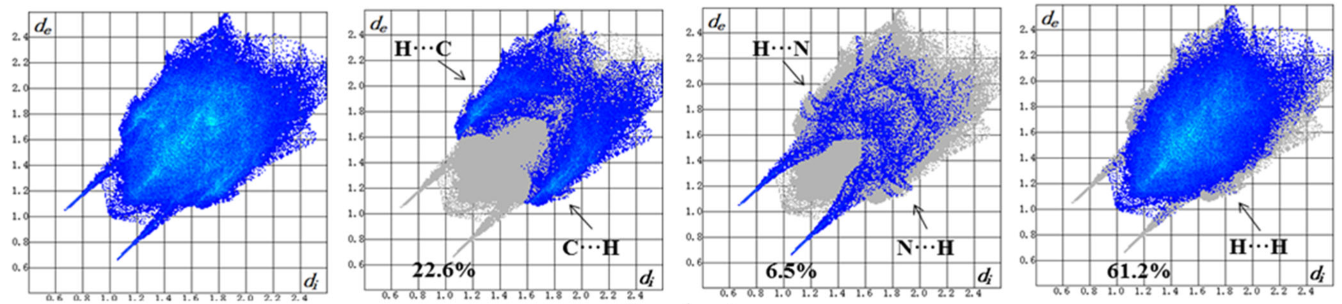

Complex **1**

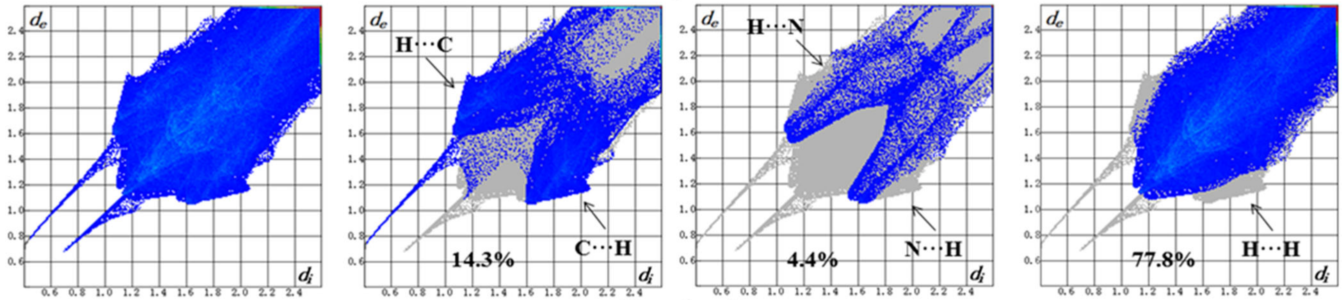

Complex **2**

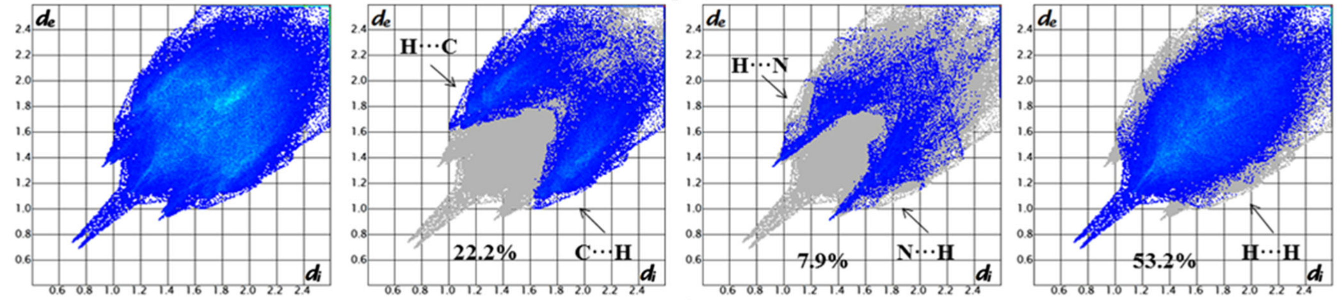

Complex **3**

FIGURE 15 Fingerprint plot: full and resolved into C···H/H···C, N···H/H···N and H···H contacts contributing to the total Hirshfeld surface area of complexes **1**, **2** and **3**

two pairs of intermolecular C–H···π (C14–H14···Cg3 and C36–H36···Cg4) hydrogen bonding interactions (Figure 9). Furthermore, every molecule links other molecules via intermolecular C–H···π hydrogen bonds forming an infinite three-dimensional supramolecular network.[52–54] The hydrogen bonding parameters are summarized in Table S4.

2.5 | Crystal structure of complex 3

The structure of complex **3** is presented in Figure 10. Selected bond lengths and angles are given in Table S5. The complex $[Cu_4(L^2)_4]\cdot 2CHCl_3$ was isolated, and crystallizes in the triclinic system, space group *P*-1, which comprises four Cu(II) atoms, four fully deprotonated $(L^2)^{2-}$ units and two crystallization chloroform molecules. The center Cu1 atom is tetra-coordinated in a N_2O_2 plane by two oxime nitrogen atoms (N3, N6) and two oxygen atoms (O1, O5) of the two deprotonated $(L^2)^{2-}$ units. The Cu(II) atom can be best described as adopting a slightly distorted square planar geometry with CuN_2O_2 coordination. Since there are very weak interactions in the axial positions with Cu2–O3 of 2.789(1) Å, the interaction between them can be neglected. Therefore, the center Cu2 atom is also tetra-coordinated by two oxime nitrogen atoms (N7, N10) and two oxygen atoms (O7, O8) of two fully deprotonated $(L^2)^{2-}$ units. The axial Cu–O and Cu–N distances are in the range 1.900(3)–1.987(7) and 1.833(7)–2.004(4) Å, respectively. Additionally, dihedral angles between the basal planes (N_2O_2 plane) and another basal plane (N_2O_2 plane) are 84.38(2)°. It can be seen that the base plane of Cu1 and the equatorial plane of Cu2 are almost perpendicular. The dihedral angle of planes N3–Cu1–O1 and O5–Cu1–N6 is 20.54(2)°. This structure may be stabilized by the intermolecular contacts (2.883(5) Å) between copper and nitrogen atoms to form a head-to-tail dimer. Unlike previous reports, solvent molecules did not participate in the coordination[55] and formed a new complex **3**.

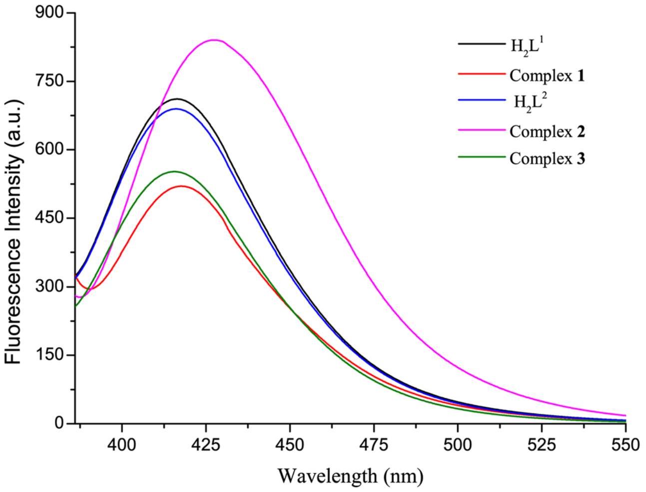

FIGURE 16 Emission spectra of H_2L^1 and H_2L^2 (λ_{ex} = 360 nm) and their complexes **1**, **2** and **3** in dilute DMF solution

Meanwhile, in the crystal structure of complex **3**, there are nine significant intramolecular hydrogen bonds (Figure 11). As illustrated in Figure 12, complex **3** molecules form an infinite three-dimensional supramolecular structure by intermolecular hydrogen bondings,[52–54] three pairs of intermolecular hydrogen bonds (C20–H20···Cl2, C45–H45C···N2 and C75–H75···O8) being formed. In addition, complex **3** molecules form a one-dimensional infinite chain structure via C–H···π and π···π (Cg3···Cg3) (Cg3 = N1–N2–C7–C8–C9) stacking interactions (Figure 13). Hydrogen bonding interactions are detailed in Table S6.

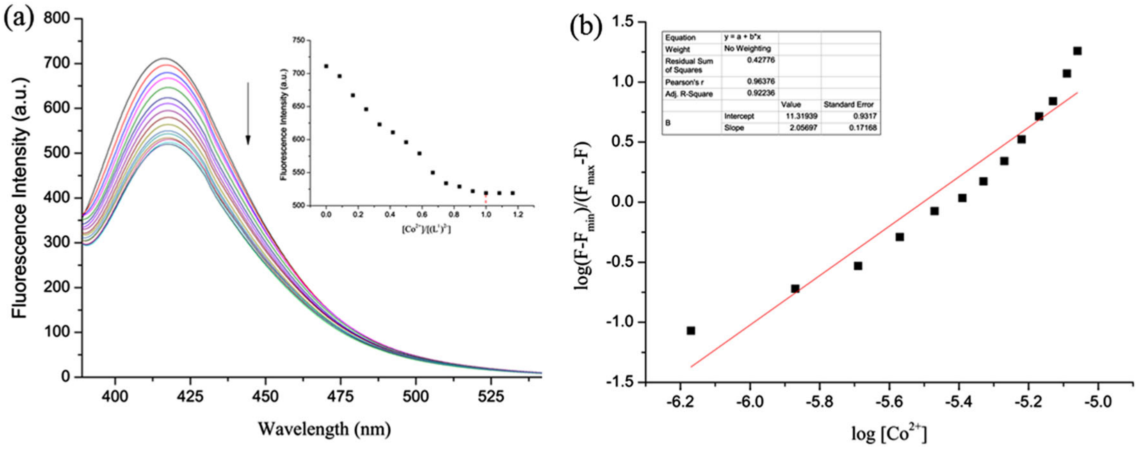

Equation	y = a + b*x		
Weight	No Weighting		
Residual Sum of Squares	0.42776		
Pearson's r	0.96376		
Adj. R-Square	0.92236		
		Value	Standard Error
B	Intercept	11.31939	0.9317
	Slope	2.05697	0.17168

FIGURE 17 (a) Fluorescence spectral changes of H_2L^1 solution upon addition of different amounts of Co(II) ions (0–1.0 equiv.) in DMF solution. Inset: the absorbance at 415 nm varied as a function of $[Co^{2+}]/[(L^1)^{2-}]$. (b) Linear relationship between fluorescence intensities and concentrations of Co(II) ions (λ_{ex} = 360 nm)

2.6 | Hirshfeld surface analyses

The Hirshfeld surfaces[56,57] of complexes **1**, **2** and **3** are depicted in Figure 14. This figure demonstrates the surface which has been mapped over d_{norm}, shape_index and curvedness. In complexes **1**, **2** and **3**, the main interactions are between the H···H, C···H/H···C and N···H/H···N surfaces, which are evident on the Hirshfeld surface, as shown by the bright red spots on the d_{norm} surface in Figure 14. However, there are several other visible spots on the Hirshfeld surface.

Two-dimensional fingerprint plots[58] of Hirshfeld surfaces for the H···H, C···H/H···C and N···H/H···N interactions are illustrated in Figure 15. These are an important supplement for the Hirshfeld surface. In addition, tkey can quantitatively describe the properties and types of intermolecular interactions between crystals. The extents of C···H/H···C interactions cover 22.6, 14.3 and 22.2% and N···H/H···N interactions cover 6.5, 4.4 and 7.9% of the total Hirshfield surfaces for complexes**1**, **2** and **3**, respectively. Whereas H···H interactions comprise 61.2, 77.8 and 53.2% of the total Hirshfeld surfaces for complexes **1**, **2** and **3**, respectively. Because there are more hydrogen atoms in the crystal structures and most of them are short-range actions, the interaction between H···H is the greatest, which is similar to previously reported complexes.[59] As a result of the existence of these hydrogen bondings, complexes **1**, **2** and **3** could be more stabilized.

2.7 | Fluorescence spectra

The fluorescence properties of H_2L^1 and H_2L^2 and their complexes were determined at room temperature. The spectra are shown in Figure 16. The free ligands H_2L^1 and H_2L^2 demonstrated an intense emission peak at *ca* 416 nm upon excitation at *ca* 360 nm, which could be attributed to intra-ligand π–π^* transition.[60,61]

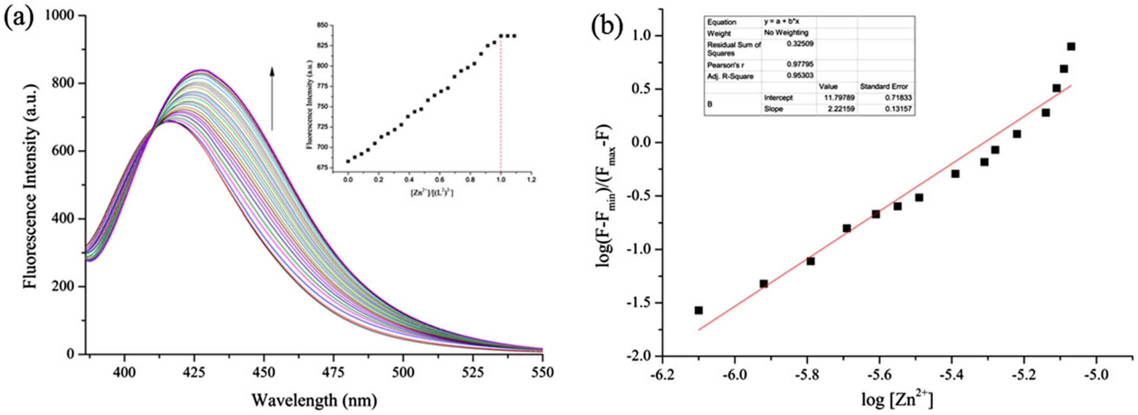

FIGURE 18 (a) Fluorescence spectral changes of H_2L^2 solution upon addition of different amounts of Zn(II) ions (0–1.0 equiv.) in DMF solution. Inset: the absorbance at 415 nm varied as a function of $[Zn^{2+}]/[(L^2)^{2-}]$. (b) Linear relationship between fluorescence intensities and concentrations of Zn(II) ions (λ_{ex} = 360 nm)

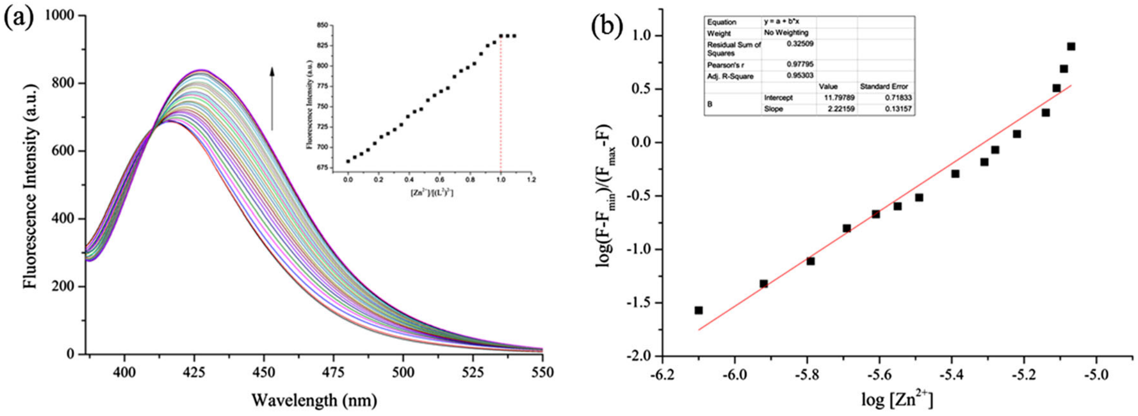

FIGURE 19 (a) Fluorescence spectral changes of H_2L^2 solution upon addition of different amounts of Cu(II) ions (0–1.0 equiv.) in DMF solution. Inset: the absorbance at 415 nm varied as a function of $[Cu^{2+}]/[(L^2)^{2-}]$. (b) Linear relationship between fluorescence intensities and concentrations of Cu(II) ions (λ_{ex} = 360 nm)

Complexes **1** and **2** demonstrated weak photoluminescence with maximum emission peaks at *ca* 516 and 510 nm upon excitation at 360 nm, respectively, However, complex **3** displayed enhanced emission intensities compared to the corresponding ligand H_2L^2, and the peaks are bathochromically shifted, which could be

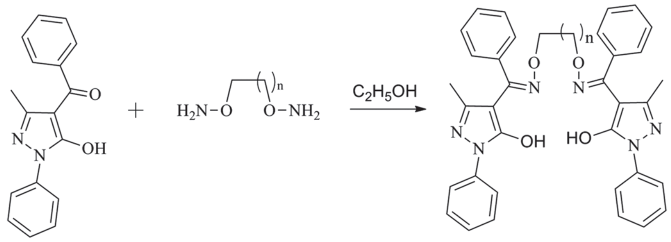

H_2L^1, n=1
H_2L^2, n=2

SCHEME 1 Synthetic route to ligands H_2L^1 and H_2L^2

TABLE 1 Crystallographic data and refinement parameters for complexes **1**, **2** and **3**

Parameter	1	2	3
Empirical formula	$C_{38}H_{38}CoN_6O_6$	$C_{114}H_{114}N_{18}O_{18}Zn_3$	$C_{150}H_{130}Cl_6Cu_4N_{24}O_{16}$
Formula weight	733.69	2220.34	2991.63
T (K)	173.00(10)	296.15	173.00(10)
Wavelength (Å)	0.71073	0.71073	0.71073
Crystal system	Triclinic	Trigonal	Triclinic
Space group	*P*-1	*R*3	*P*-1
a (Å)	9.2446(14)	20.2381(11)	13.3304(11)
b (Å)	12.512(2)	20.2381(11)	13.9358(11)
c (Å)	15.8811(18)	31.3312(15)	21.7616(15)
α (°)	81.798(11)	90	108.544(7)
β (°)	78.146(11)	90	94.920(6)
γ (°)	70.492(14)	120	104.045(7)
V (Å^3)	1689.1(5)	1689.1(5)	3659.3(5)
Z	2	3	1
D_{calc} (g cm^{-3})	1.447	0.995	1.358
μ (mm^{-1})	0.567	0.537	0.754
F (000)	766.0	3474	1544
Crystal size (mm)	0.21 × 0.17 × 0.14	0.22 × 0.19 × 0.18	0.23 × 0.21 × 0.17
θ range (°)	3.349–26.022	2.413–25.387	3.253–26.022
Index ranges	$-11 \leq h \leq 10$ $-15 \leq k \leq 15$ $-19 \leq l \leq 19$	$-24 \leq h \leq 24$ $-23 \leq k \leq 24$ $-35 \leq l \leq 37$	$-16 \leq h \leq 16$ $-17 \leq k \leq 17$ $-21 \leq l \leq 26$
Reflections collected	11612	27932	25981
Unique reflections	6650	8813	14395
R_{int}	0.0809	0.0858	0.0600
Completeness (%) (θ)	99.7 (25.242)	99.9 (25.242)	99.7 (25.242)
Data/restraints/parameters	6650/6/470	8813/871/430	14395/90/1007
Goodness of fit (GOF)	1.058	1.035	1.038
Final R_1, wR_2 indices	0.0768, 0.1163	0.0650, 0.1529	0.0776, 0.1754
R_1, wR_2 indices (all data)	0.1422, 0.1586	0.0893, 0.1663	0.1340, 0.2222
Residuals peak/hole (e Å^{-3})	0.916 and −0.480	0.737 and −0.460	1.340 and −0.675

attributed to ligand-to-metal charge transfer.[62] In addition, fluorescence titration experiments of complexes **1**, **2** and **3** were conducted in DMF solution (1.0×10^{-5} M). The results are shown in Figures 17, 18 and 19. It can be seen from the fluorescence spectra that the fluorescence intensities gradually change when different metal ions are gradually added. When the amount of metal ions reached 1.0 equiv., the fluorescence emission intensity remained relatively constant. Furthermore, from the emission intensity by following the modified Benesi–Hidebrand equation, the association constants of complexes **1**, **2** and **3** were calculated as 2.98×10^5, 1.67×10^5 and 3.69×10^5 M^{-1}.[19,21]

3 | CONCLUSIONS

In summary, three new metal complexes with symmetric N_2O_2-donors ligands were successfully prepared and characterized. X-ray crystal structure analyses revealed the Co(II) and Zn(II) atoms of complexes **1** and **2** are hexacoordinated and adopt slightly distorted octahedral coordination geometries. Complexes **1**, **2** and **3** possess self-assembling infinite two-, three- and three-dimensional supramolecular structures via intermolecular hydrogen bonding and C–H···π and π···π stacking interactions, respectively. The intermolecular interactions of the two complexes were discussed in terms of Hirshfeld surface analyses and two-dimensional fingerprint plots. In addition, fluorescence behaviors of the ligands H_2L^1 and H_2L^2 were studied. Compared with the ligands H_2L^1 and H_2L^2, the luminescence intensities of complexes **1** and **3** decreased significantly. However, the luminescence intensity of complex **2** increased significantly, indicating that the different ions have different fluorescence effects.

4 | EXPERIMENTAL

4.1 | Materials and physical measurements

1-Phenyl-3-methyl-4-benzoyl-5-pyrazolone (PMBP) from East China Normal University Chemical Plant was used without further purification. The other reagents and solvents were analytical grade reagents from Tanjin Chemical Reagent Factory.

C, H and N analyses were obtained using a VariuoEL V3.00 automatic elemental analysis instrument. Elemental analyses for Co(II), Zn(II) and Cu(II) were conducted with an IRIS ER/S-WP–1 ICP atomic emission spectrometer. Melting points were obtained by the use of a microscopic melting point apparatus (Beijing Taike Instrument Company Limited) and were uncorrected. IR spectra (400–4000 cm^{-1}) were recorded using a Vertex 70 FT-IR spectrophotometer, with samples prepared as KBr pellets. UV–visible absorption spectra were recorded with a Shimadzu UV-3900 spectrometer. ^1H NMR spectra were obtained with an AVANCE DRX-400/600 spectrometer (Bruker, Germany). X-ray single-crystal structure determinations for complexes **1**, **2** and **3** were carried out with SuperNova Dual (Cu at zero) or Bruker APEX-II CCD diffractometers. Fluorescence spectra were recorded with an F-7000 FL spectrophotometer.

4.2 | Synthesis of H_2L

1,2-Bis(aminooxy)ethane and 1,3-bis(aminooxy)propane were prepared according to an analogous method reported earlier.[63] The symmetric N_2O_2-type ligand H_2L was synthesized according to the procedures reported in earlier literature.[64,65] The major synthetic route to ligands H_2L^1 and H_2L^2 is shown in Scheme 1.

4.2.1 | Synthesis of H_2L^1

To an ethanol solution (15 ml) of PMBP (531.2 mg, 1.91 mmol) was added an ethanol solution (5 ml) of 1,2-bis(aminooxy)ethane (124.6 mg, 1.35 mmol). The mixed solution was stirred at 55°C for 10 h. After cooling to room temperature, the precipitates were collected. The product was dried *in vacuo*, and a colorless solid was obtained (Scheme 1). Yield: 493.2 mg, 75.2%. M.p. 201–203°C. Anal. calcd for $C_{36}H_{32}N_6O_4$ (%): C, 70.57; H, 5.26; N, 13.72. Found (%): C, 70.64; H, 5.47; N, 13.58.

4.2.2 | Synthesis of H_2L^2

To an ethanol solution (15 ml) of PMBP (917.4 mg, 3.30 mmol) was added an ethanol solution (5 ml) of 1,3-bis(aminooxy)propane (241.3 mg, 2.28 mmol). The mixed solution was stirred at 55°C for 10 h. After cooling to room temperature, the precipitates were collected. The product was dried *in vacuo*, and a colorless solid was obtained (Scheme 1). Yield: 827.3 mg, 71.4%. M.p. 196–197°C. Anal. calcd for $C_{37}H_{34}N_6O_4$ (%): C, 70.91; H, 5.47; N, 13.41. Found (%): C, 70.82; H, 5.61; N, 13.57.

4.3 | Syntheses of complexes

4.3.1 | Synthesis of complex 1

A methanolic solution (3 ml) of $Co(OAc)_2 \cdot 4H_2O$ (3.48 mg, 0.01 mmol) was gradually added to a chloroform solution (2 ml) of H_2L^1 (6.16 mg, 0.01 mmol). A bright brown solution was obtained. The reaction solution was stirred for 10 min at room temperature. Several brown needle-like single crystals suitable for X-ray analysis were obtained by slow evaporation of the maternal solution in a bottle after one week. They were separated and washed several times with cold methanol and dried *in vacuo*. Yield: 58.3%. Anal. calcd for $C_{38}H_{38}CoN_6O_6$ (%): C, 62.21; H, 5.22; N, 11.45; Co, 8.03. Found (%): C, 61.87; H, 5.54; N, 11.59; Co, 7.89.

4.3.2 | Synthesis of complex 2

A solution of $Zn(NO_3)_2{\cdot}6H_2O$ (2.97 mg, 0.010 mmol) in methanol (2 ml) was added to a solution of ligand H_2L^2 (6.26 mg, 0.010 mmol) in methanol (2 ml). The mixed solution was kept stirring for 10 min, and gently heated to 60°C, the color of the mixed solution gradually clarifying. After cooling to room temperature and then filtering, the filtrate was allowed to stand for a few days in the dark at room temperature. Colorless block-shaped single crystals suitable for X-ray diffraction measurements were formed at the bottom of the bottle after a few days on slow evaporation of solvent. Yield: 50.8%. Anal. calcd for $C_{114}H_{114}N_{18}Zn_3O_{18}$ (%): C, 61.67; H, 5.18; N, 11.35; Zn, 8.83. Found (%): C, 61.45; H, 5.33; N, 11.19; Zn, 8.94.

4.3.3 | Synthesis of complex 3

A methanol solution (2 ml) of $Cu(OAc)_2{\cdot}2H_2O$ (1.99 mg, 0.01 mmol) was added to a chloroform solution (3 ml) of ligand H_2L^2 (6.26 mg, 0.01 mmol), and the color of the mixed solution immediately turned brown. The reaction solution was stirred for 10 min at room temperature, and the mixture solution was filtered and the filtrate was allowed to stand for a few days in the dark. Several brown needle-like single crystals suitable for X-ray analysis were obtained by slow evaporation of the maternal solution in the bottle. Yield: 53.7%. Anal. calcd for $C_{150}H_{130}Cl_6Cu_4N_{24}O_{16}$ (%): C, 60.22; H, 4.38; N, 11.24; Cu, 8.50. Found(%): C, 60.13; H, 4.54; N, 11.49; Cu, 8.36.

4.4 | Crystal structure determinations of complexes

Crystal data of complexes **1**, **2** and **3** were collected with a SuperNova Dual Eos (Cu at zero) or Bruker APEX-II CCD diffractometer equipped with a graphite monochromator and Mo Kα ($\lambda = 0.71073$ Å) radiation. The LP corrections were applied to the SAINT program and semi-empirical corrections were applied to the SADABS program. The structures of complexes **1**, **2** and **3** were solved using the direct method with SHELXS-2014.[66] All hydrogen atoms were added theoretically and difference-Fourier map exhibited the positions of the remaining atoms. The hydrogen atoms were placed in idealized positions and constrained to ride on their parent atoms. All the non-hydrogen atoms were refined with independent anisotropic displacement parameters using a full-matrix least-squares procedure on F^2 with SHELXL-2014.[67] The crystal data and experimental parameters relevant to the structure determinations are listed in Table 1.

ACKNOWLEDGEMENTS

This work was supported by the National Natural Science Foundation of China (21761018) and the Program for Excellent Team of Scientific Research in Lanzhou Jiaotong University (201706), both of which are gratefully acknowledged.

SUPPLEMENTARY MATERIAL

CCDC 1890720–1890722 contain the supplementary crystallographic data for complexes **1**, **2** and **3**. These data can be obtained free of charge via http://www.ccdc.cam.ac.uk/conts/retrieving.html, or from the Cambridge Crystallographic Data Centre, 12 Union Road, Cambridge CB2 1EZ, UK; fax: (+44) 1223 336 033; or e-mail: deposit@ccdc.cam.ac.uk.

ORCID

Wen-Kui Dong https://orcid.org/0000-0003-1249-5808

REFERENCES

[1] L. Gao, F. Wang, Q. Zhao, Y. Zhang, W. K. Dong, *Polyhedron* **2018**, *139*, 7.

[2] L. Zhao, X. T. Dong, Q. Cheng, J. X. Zhao, L. Wang, *Synth. React. Inorg. Met.-Org. Nano-Met. Chem.* **2013**, *43*, 1241.

[3] P. Wang, L. Zhao, *Spectrochim. Acta A* **2015**, *342*, 135.

[4] J. Q. Guo, Y. X. Sun, B. Yu, J. Li, H. R. Jia, *Chin. J. Inorg. Chem.* **2017**, *33*, 1481.

[5] J. Li, H. J. Zhang, J. Chang, H. R. Jia, Y. X. Sun, Y. Q. Huang, *Crystals* **2018**, *8*, 176.

[6] X. Y. Dong, Y. X. Sun, L. Wang, L. Li, *J. Chem. Res.* **2012**, *36*, 387.

[7] X. Y. Li, Q. P. Kang, L. Z. Liu, J. C. Ma, W. K. Dong, *Crystals* **2018**, *8*, 43.

[8] H. L. Wu, C. P. Wang, F. Wang, H. P. Peng, H. Zhang, Y. C. Bai, *J. Chin. Chem. Soc.* **2015**, *62*, 1028.

[9] H. L. Wu, Y. C. Bai, Y. H. Zhang, Z. Li, M. C. Wu, C. Y. Chen, J. W. Zhang, *J. Coord. Chem.* **2014**, *67*, 3054.

[10] H. L. Wu, G. L. Pan, Y. C. Bai, H. Wang, J. Kong, F. R. Shi, Y. H. Zhang, X. L. Wang, *J. Chem. Res.* **2014**, *38*, 211.

[11] H. L. Wu, H. Wang, X. L. Wang, G. L. Pan, F. R. Shi, Y. H. Zhang, Y. C. Bai, J. Kong, *New J. Chem.* **2014**, *38*, 1052.

[12] H. L. Wu, G. L. Pan, Y. C. Bai, H. Wang, J. Kong, F. R. Shi, Y. H. Zhang, X. L. Wang, *Res. Chem. Intermed.* **2015**, *41*, 3375.

[13] L. Q. Chai, L. J. Tang, L. C. Chen, J. J. Huang, *Polyhedron* **2017**, *122*, 228.

[14] L. Q. Chai, K. Y. Zhang, L. J. Tang, J. Y. Zhang, H. S. Zhang, *Polyhedron* **2017**, *130*, 100.

[15] Y. D. Peng, X. Y. Li, Q. P. Kang, G. X. An, Y. Zhang, W. K. Dong, *Crystals* **2018**, *8*, 1079.

[16] Y. J. Dong, X. L. Li, Y. Zhang, W. K. Dong, *Supramol. Chem.* **2017**, *29*, 518.

[17] B. Yu, C. Y. Li, Y. X. Sun, H. R. Jia, J. Q. Guo, J. Li, *Spectrochim. Acta A* **2017**, *184*, 249.

[18] B. J. Wang, W. K. Dong, Y. Zhang, S. F. Akogun, *Sens. Actuators B* **2017**, *247*, 254.

[19] F. Wang, L. Gao, Q. Zhao, Y. Zhang, W. K. Dong, Y. J. Ding, *Spectrochim. Acta A* **2018**, *190*, 111.

[20] W. K. Dong, S. F. Akogun, Y. Zhang, Y. X. Sun, X. Y. Dong, *Sens. Actuators B* **2017**, *238*, 723.

[21] J. Hao, X. Y. Li, Y. Zhang, W. K. Dong, *Materials* **2018**, *11*, 523.

[22] Q. P. Kang, X. Y. Li, Q. Zhao, J. C. Ma, W. K. Dong, *Appl. Organometal. Chem.* **2018**, *32*, e4379.

[23] L. Gao, C. Liu, F. Wang, W. K. Dong, *Crystals* **2018**, *8*, 77.

[24] H. R. Jia, J. Chang, H. J. Zhang, J. Li, Y. X. Sun, *Crystals* **2018**, *8*, 272.

[25] Y. X. Sun, C. Y. Li, C. J. Yang, Y. Y. Zhao, J. Q. Guo, B. Yu, *Chin. J. Inorg. Chem.* **2016**, *32*, 327.

[26] L. W. Zhang, L. Z. Liu, F. Wang, W. K. Dong, *Molecules* **2018**, *23*, 1141.

[27] D. J. Darensbourg, *Chem. Rev.* **2007**, *107*, 2388.

[28] X. Y. Dong, X. Y. Li, L. Z. Liu, H. Zhang, Y. J. Ding, W. K. Dong, *RSC Adv.* **2017**, *7*, 48394.

[29] L. H. Li, W. K. Dong, Y. Zhang, S. F. Akogun, L. Xu, *Appl. Organometal. Chem.* **2017**, *31*, e3818.

[30] W. K. Dong, J. C. Ma, Y. J. Dong, L. C. Zhu, Y. Zhang, *Polyhedron* **2016**, *115*, 228.

[31] P. P. Liu, L. Sheng, X. Q. Song, W. Y. Xu, Y. A. Liu, *Inorg. Chim. Acta* **2015**, *434*, 252.

[32] X. Q. Song, P. P. Liu, Z. R. Xiao, X. Li, Y. A. Liu, *Inorg. Chim. Acta* **2015**, *438*, 232.

[33] Y. A. Liu, C. Y. Wang, M. Zhang, X. Q. Song, *Polyhedron* **2017**, *127*, 278.

[34] W. K. Dong, J. C. Ma, L. C. Zhu, Y. Zhang, *Cryst. Growth Des.* **2016**, *16*, 6903.

[35] X. Y. Dong, Q. P. Kang, X. Y. Li, J. C. Ma, W. K. Dong, *Crystals* **2018**, *8*, 139.

[36] Y. D. Peng, F. Wang, L. Gao, W. K. Dong, *J. Chin. Chem. Soc.* **2018**, *65*, 893.

[37] F. Wang, L. Z. Liu, L. Gao, W. K. Dong, *Spectrochim. Acta A* **2018**, *203*, 56.

[38] W. K. Dong, J. Zhang, Y. Zhang, N. Li, *Inorg. Chim. Acta* **2016**, *444*, 95.

[39] X. Y. Dong, Q. Zhao, Z. L. Wei, H. R. Mu, H. Zhang, W. K. Dong, *Molecules* **2018**, *23*, 1006.

[40] Y. J. Dong, X. Y. Dong, W. K. Dong, Y. Zhang, L. S. Zhang, *Polyhedron* **2017**, *123*, 305.

[41] Z. L. Ren, J. Hao, P. Hao, X. Y. Dong, Y. Bai, W. K. Dong, *Z. Naturforsch.* **2018**, *73*, 203.

[42] W. K. Dong, L. C. Zhu, Y. J. Dong, J. C. Ma, Y. Zhang, *Polyhedron* **2016**, *117*, 148.

[43] L. Wang, J. C. Ma, W. K. Dong, L. C. Zhu, Y. Zhang, *Z. Anorg. Allg. Chem.* **2016**, *642*, 834.

[44] S. Akine, T. Taniguchi, W. K. Dong, S. Masubuchi, T. Nabeshima, *J. Org. Chem.* **2005**, *70*, 1704.

[45] X. Y. Li, L. Chen, L. Gao, Y. Zhang, S. F. Akogun, W. K. Dong, *RSC Adv.* **2017**, *7*, 35905.

[46] W. K. Dong, S. S. Zheng, J. T. Zhang, Y. Zhang, Y. X. Sun, *Spectrochim. Acta A* **2017**, *184*, 141.

[47] L. Wang, Q. P. Kang, J. Hao, W. K. Dong, *Chin. J. Inorg. Chem.* **2018**, *34*, 525.

[48] L. Wang, X. Y. Li, Q. Zhao, L. H. Li, W. K. Dong, *RSC Adv.* **2017**, *7*, 48730.

[49] J. Hao, L. H. Li, J. T. Zhang, S. F. Akogun, L. Wang, W. K. Dong, *Polyhedron* **2017**, *134*, 1.

[50] H. Zhang, W. K. Dong, Y. Zhang, S. F. Akogun, *Polyhedron* **2017**, *133*, 279.

[51] C. H. Tao, J. C. Ma, L. C. Zhu, Y. Zhang, W. K. Dong, *Polyhedron* **2017**, *128*, 38.

[52] H. J. Zhang, J. Chang, H. R. Jia, Y. X. Sun, *Chin. J. Inorg. Chem.* **2018**, *34*, 2261.

[53] Y. X. Sun, Y. Y. Zhao, C. Y. Li, B. Yu, J. Q. Guo, J. Li, *Chin. J. Inorg. Chem.* **2016**, *32*, 913.

[54] J. Chang, H. J. Zhang, H. R. Jia, Y. X. Sun, *Chin. J. Inorg. Chem.* **2018**, *34*, 2097.

[55] W. K. Dong, J. F. Tong, Y. X. Sun, J. C. Wu, J. Yao, S. S. Gong, *Transition Met. Chem.* **2010**, *35*, 419.

[56] A. D. Martin, K. J. Hartlieb, A. N. Sobolev, C. L. Raston, *Cryst. Growth Des.* **2010**, *10*, 5302.

[57] M. A. Spackman, J. J. McKinnon, D. Jayatilaka, *CrystEngComm* **2008**, *10*, 377.

[58] A. L. Rohl, M. Moret, W. Kaminsky, K. Claborn, J. J. Mckinnon, B. Kahr, *Cryst. Growth Des.* **2008**, *8*, 4517.

[59] Q. Evrard, C. Leuvrey, P. Farger, E. Delahaye, P. Rabu, G. Taupier, K. D. Dorkenoo, J. M. Rueff, N. Barrier, O. Perez, G. Rogez, *Cryst. Growth Des.* **2018**, *18*, 1809.

[60] L. Xu, L. C. Zhu, J. C. Ma, Y. Zhang, J. Zhang, W. K. Dong, *Z. Anorg. Allg. Chem.* **2015**, *641*, 2520.

[61] L. Chen, W. K. Dong, H. Zhang, Y. Zhang, Y. X. Sun, *Cryst. Growth Des.* **2017**, *17*, 3636.

[62] J. C. Ma, X. Y. Dong, W. K. Dong, Y. Zhang, L. C. Zhu, J. T. Zhang, *J. Coord. Chem.* **2016**, *69*, 149.

[63] S. Akine, T. Taniguchi, T. Nabeshima, *Chem. Lett.* **2001**, *30*, 682.

[64] S. Akine, W. K. Dong, T. Nabeshima, *Inorg. Chem.* **2006**, *45*, 4677.

[65] L. Wang, J. Hao, L. X. Zhai, Y. Zhang, W. K. Dong, *Crystals* **2017**, *7*, 277.

[66] G. M. Sheldrick, SHELXS-2014, Program for the solution of crystal structures, University of Göttingen, Germany, **2014**.

[67] G. M. Sheldrick, SHELXL-2014, Program for the refinement of crystal structures, University of Göttingen, Germany, **2014**.

SUPPORTING INFORMATION

Additional supporting information may be found online in the Supporting Information section at the end of the article.

How to cite this article: Kang Q-P, Li X-Y, Wang L, Zhang Y, Dong W-K. Containing-PMBP N_2O_2-donors transition metal(II) complexes: Synthesis, crystal structure, Hirshfeld surface analyses and fluorescence properties. *Appl Organometal Chem*. 2019;e5013. https://doi.org/10.1002/aoc.5013